TASK CONSTRAINTS ACT AT THE LEVEL OF SYNERGIES AND AT THE LEVEL OF END-EFFECTOR KINEMATICS IN MANUAL REACHING AND MANUAL LATERAL INTERCEPTION

Inge Tuitert, Laura Golenia,
Egbert Otten, Reinoud J. Bootsma,
Raoul M. Bongers

Submitted

Abstract

To coordinate the redundant degrees of freedom (DOF) in the action system, synergies are often proposed. Synergies organize DOF in temporary task-specific units emerging from interactions amongst task, organism, and environmental constraints. We examined whether task constraints affect synergies, end-effector kinematics, or both. To this end, we compared synergies and end-effector kinematics when participants (N = 15) performed discrete movements of identical amplitude in manual reaching (stationary targets) and manual lateral interception (moving targets, with different angles of approach). We found that time-velocity profiles were roughly symmetric in reaching, whereas they had a longer decelerative tail and showed an angle-of-approach effect in interception. Uncontrolled Manifold analyses showed that in all conditions joint angle variability was primarily co-variation, indicating a synergistic organization. The analysis on the clusters of joint angle configurations used in the conditions demonstrated differences between reaching and interception synergies, whereas similar synergies were used within interception conditions. This implies that some task constraints operate at the level of synergies while other task constraints only affect end-effector kinematics. The results support a two-step process in the organization of DOF, consisting of synergy formation and further constraining of synergies to produce the actual movement, as proposed by Kay [10].

Introduction

Central in the domain of motor control research is the degrees of freedom (DOF) problem [1]. The core of this problem is that the number of DOF (e.g., joint angles) used to perform a goal-directed activity usually exceeds the minimum necessary (cf. [9,13,109]). To illustrate this, think of a planar arm with three joints keeping the end-effector at a target. Here, the three joint angles describe the joint configuration of the arm, while two coordinates describe the position of the end-effector in the plane. Because the number of DOF at joint level exceeds that at end-effector level, various joint angle configurations result in the same end-effector position. This so-called redundancy raises a key concern in studies of motor control questioning how the redundant DOF are coordinated to perform goal-directed actions (cf. [1,110]). A coordinative principle suggested by Bernstein [1] proposes how DOF are linked in a synergy. This suggestion inspired different approaches to gain a deeper understanding on the functioning of synergies over the last four decades (for pertinent overviews see [3,4,111,112]). In the current paper, we studied synergies from the dynamical systems perspective to movement coordination that understands synergies as flexible assemblies of DOF. Synergies are thus considered to be temporary organizations of DOF to perform a specific task or function. These synergies emerge from interactions amongst task, organism, and environmental constraints in a self-organizing manner [3,13,25,26,110,112,113]. To understand the role of constraints in the formation of these synergies and their role in producing the resulting goal-directed behaviour, we examined whether different synergies emerged as a function of task constraints.

To do this, we took the proposal of Kay [10] as a starting point. Kay assumed that once the DOF are linked into a synergy (based on the interactions between task, organism, and environmental constraints), more specific constraints confine the synergy to produce the actual movement. Thus, constraints are proposed to act at two levels during the process of emerging behavior [10,26,29]; constraints act (i) on the DOF to form an emergent synergy and, (ii) on the synergy to produce the actual behavior. To illustrate this, we consider the example of manual lateral interception, where the end-effector moves along a lateral displacement axis so as to intercept an approaching target that, over different trials, may follow different trajectories (different angles of approach) to the same interception position (e.g., [53]). The fact that a discrete movement has to be made could be one of the constraints that acts on the DOF, leading to the emergence of the synergy that can move the hand laterally. The target's angle of approach (and other constraints for that matter) may further constrain the synergy giving rise to the specifics of the movement to intercept the target (i.e., end-effector kinematics). Taking Kay's two-step framework as a starting point, we examined the effect of changes in task constraints on emergent synergies and end-effector kinematics to establish the tasks and conditions in which different synergies were used.

Two notions are of importance to gauge emergent synergies. First, within an emergent synergy variation in one DOF is compensated for in other DOF so that task performance is stabilized (cf. [3,4,18,26–28,32,33]). In terms of pointing at a target this means that a change in one joint angle is compensated by changes in one or more other joint angle(s) to preserve the position of the end-effector, that is, there is co-variation amongst joint angles. Therefore, we take the degree of co-variation to characterize the synergistic organization of

DOF. Second, although there is a wide variety of configurations of DOF with which a given task can be performed, usually only a subset of these configurations is exploited. Think again about our example where an end-effector points at a target; here, there are many joint angle configurations that keep the end-effector at the target. Usually, not all of these options are employed: over repetitions of the same task, people typically only use a limited set of the available options of suitable joint angle configurations. Arguably, the total set of suitable configurations interacts with other constraints in the task, organism, and environment to form the synergy for that task. The subset or cluster of joint angle configurations actually used in positioning the end-effector, which has a certain location and size in joint space, emerges from these interactions and reflects the synergy (cf. Profeta & Turvey, 2018). In the current paper, the degree of co-variation in DOF as well as the cluster of DOF configurations used are examined to compare and characterize synergies.

A method to examine these aspects of synergistic organization of DOF is the Uncontrolled Manifold (UCM) analysis [4,32,33]. This analysis partitions variability in DOF across repetitions of trials into two types. The first type of variability is variability within the set of DOF configurations that stabilizes a performance variable (i.e., co-variation), that is, variability in joint angles that does not affect end-effector position. The other type of variability in DOF leads to deviations of the performance variable, that is, joint angle variability moving the end-effector away from a certain position. The variability in DOF not affecting the end-effector position (i.e., co-variation) should be larger than the variability in DOF affecting the end-effector position to execute a given task. Therefore, we use the degree of co-variation as a measure to assess synergistic organization of DOF. In addition, a variation on an adapted version of the UCM method ([115] see also, [87]) will be used in the current study to compare the location and size in joint space of the clusters of employed joint angle configurations between tasks and among conditions within one task. These clusters of joint angle configurations are taken to reflect the subset from the total set of suitable joint angle configurations employed by the synergies.

We applied these methods in two tasks involving the upper extremity where task constraints related to timing and guidance towards the target were varied. The two tasks were manual reaching and manual lateral interception, bringing the end-effector toward identical target (arrival) positions. In the manual reaching task, participants moved the tip of the index-finger from a start position to a stationary target position, in the lateral direction, by sliding the end-effector along a lateral axis. Aside from the instruction to move as fast as possible, no particular constraints on speed or movement time were imposed. In the lateral manual interception task, participants had to intercept a moving target that approached the participant in the horizontal plane by sliding the end-effector along the same lateral axis. The moving target imposed a timing constraint and guided the movement of the index-finger to intercept the target at the arrival position. To modulate the guidance of the movement of the index-finger, we varied the target's trajectory (approach angle) to the final arrival position (e.g., [53–56]).

What is known about the use of synergies and kinematics in these two tasks? The kinematics of the end-effector have been examined extensively, yet, separately for manual reaching (e.g.,[51,52,108]) and manual lateral interception (e.g., [53–56]). In manual reaching, a main

kinematic feature is a roughly symmetric bell-shaped velocity profile [51,52] where the maximum velocity of the end-effector increases with target distance [108]. In general, the symmetry of the velocity profile is not affected by target distance [108]. In manual lateral interception, the velocity profile depends on characteristics of the trajectory of the target; for example, if the target motion duration is sufficiently long, the velocity profile demonstrates a longer deceleration tail [53]. Moreover, the angle of approach of the target influences the velocity profile of the hand to the interception location in a systematic way [53–56]. Based on these findings in the literature, we foresee differences in end-effector kinematics between tasks and amongst interception conditions. We expect that the velocity profiles of manual reaching will be roughly bell-shaped, whereas the velocity profiles in manual lateral interception are expected to have longer deceleration tails and portray an angle-of-approach effect.

The use of joint angle synergies has been studied in manual reaching; however, studies addressing this issue in interception are sparse. Using UCM analyses, it has been demonstrated that the joint angles of the arm stabilize the end-effector position (e.g. [38,43,44,66,87,115–118]), implying that the joint angles are organized in synergies in reaching. Furthermore, the range of joint angle configurations employed by a synergy has been found to be larger in specific conditions. For instance, it is higher in more challenging conditions compared to a control condition [44], and during learning it is higher at the end of learning compared to at the start [35,99], or in mid-childhood development it is higher than in adults [115,119]. In manual lateral interception, synergies have not been studied using UCM analysis. However, in other interception tasks the influence of varying task constraints on the linking of joints within a synergy has been addressed with analysis other than the UCM [120,121]. For example, in unrestrained one-handed catching of real objects with large variations in target arrival positions, the couplings amongst several joints have been quantified [120] and couplings between pairs of joints have been shown to be stronger when the objects approached faster [121]. Based on these previous findings we predict that synergies arise in both tasks used in the current study.

In summary, we asked whether different synergies are used when task constraints are varied to create different tasks and conditions in manual goal-directed reaching. We started from the assumption that task constraints act separately at the level of synergies and at the level of end-effector kinematics. Synergies were characterized by (i) the degree of co-variation amongst joint angles over repetitions of the same task and condition and (ii) the cluster of joint angle configurations that the synergy employed in a condition. Our analyses were structured in the following way. First, we tested whether the shape of the velocity profiles of the end-effector differed between manual reaching and manual interception and amongst interception conditions. Second, we investigated whether joint angles were organized in synergies in all manual reaching and manual lateral interception conditions, using the UCM analysis [4,32,33]. Third, we assessed whether synergies differed between manual reaching and manual interception and amongst interception conditions. To do this we used an adapted version of the motor equivalent analysis proposed by Schöner ([114] see also, [87]).

Methods

Participants

The sample size was estimated using G*Power (Version 3.1; [122]) based on one of the primary analysis in the current study, that is, finding a larger V_{ucm} than V_{ort}. Former studies [94,119] showed strong effects for the difference between V_{ucm} and V_{ort}. Based on this, we took a relatively more conservative effect size (f = 0.4) for sample size estimation. Fifteen participants would allow the detection of an effect at alpha = 0.05 with a power of 0.8 for a repeated-measures analysis of variance with a two-level within-subject variable. This number is in line with the number of participants included in earlier studies detecting differences between conditions in a rod reaching experiment focusing on Vucm and Vort (e.g., [66]). Therefore, we aimed at including 15 of participants.

Fifteen right-handed adults (8 males and 7 females, mean age 25 years, standard deviation 9 years) participated in the experiment. All participants had normal or corrected-to-normal vision. The study was approved by the local Ethical Board of the Center for Human Movement Sciences of the University Medical Center Groningen, Groningen, The Netherlands. Written informed consent was obtained from all participants included in the study prior to the start of the experiment.

Apparatus

Participants were seated on a chair of which the backrest was extended with a plate. The trunk of the participants was gently strapped to this plate [43,100] to prevent movements of the trunk while permitting free rotations in the shoulder joints. The chair was placed at the long edge of a table in which a flat screen television (Panasonic TH-50PY70F; screen size 110.5 x 62 cm, 1920 x 1080 m pixel resolution) was horizontally embedded. Participants rested their elbow on an arm rest at the start of each trial to standardize the starting posture as much as possible across trials.

3D positions of IREDs (infrared light-emitting diodes) attached to the body were measured at a sampling frequency of 100 Hz with two Optotrak 3020 system sensors using First Principles (Northern Digital, Waterloo, Canada). Six triangular rigid PVC plates, with each three IREDs (one in each corner of the triangle) were attached to the participant's sternum, the acromion, on the lateral side of the right upper arm below the insertion of the deltoid, proximal to the ulnar and radial styloids, to the dorsal surface of the hand [67], and to the index-finger [43], using skin-friendly tape. A small aluminum plate was taped under the index-finger to prevent flexion-extension in the interphalangeal joints while allowing for flexion-extension and adduction-abduction in the metacarpophalangeal joint. Following the procedure described by Van Andel et al. (2008), the positions of the six rigid bodies were linked to 19 local anatomical positions for each participant, using a standard pointer device. The fingertip position along the lateral axis of the television screen was also recorded using a draw-wire potentiometer (FDMK46-1000-P10, Altheris, the Netherlands). The potentiometer was placed at the left bottom of the table and its wire was attached to the fingertip with Velcro tape.

Procedure

The experiment commenced with attaching the rigid bodies to the dominant right arm and the trunk. Subsequently, the anatomical landmarks were recorded. After this procedure, the participant was strapped to the chair and the draw-wire was attached to the index-finger. In the two tasks of the experiment (reaching and interception) the starting location of the right fingertip was always aligned with the body midline at the near edge of the screen (see Figure 1). Participants were instructed to slide the index-finger along the edge of the screen during the movement towards the target in both tasks.

Reaching

A reaching trial began with the presentation of the start target and the goal target (both 1.5-cm diameter circles) at the near side of the screen. Goal targets could be located at distances of 20, 30 or 40 cm to the right of the start target (see Figure 1), all on a lateral axis at the edge of the tv screen parallel to the frontal plane. After the appearance of the targets, participants placed their index finger on the start target, with the elbow at the elbow rest, and initiated their movement at their own convenience. After movement initiation the elbow could be moved without any restrictions. The instruction for the reaching movements was to reach the goal target as fast and accurate as possible. No feedback about the performance was provided.

Interception

An interception trial started with the presentation of the start target at the near side of the screen and the goal target (diameter 2-cm circle) at the far side. After remaining at its initial position for 1.5 s, the goal target started to move across the screen towards its near side, arriving there after 1 s (orthogonal velocity 60 cm/s). The participant was instructed to initiate the interceptive action after the goal target had started to move (trials where participants moved within 150 ms after the goal target started moving were excluded to control for this). The instruction for the interceptive action was to intercept the goal target by moving the fingertip along the lateral axis reaching low velocity at the instant of interception. Goal target arrival positions on the interception axis were identical to those used in the reaching task (20, 30, and 40 cm to the right of the start target). The goal target could arrive at these arrival positions with one of the three angles of approach (-26.5°, 0°, 26.5°; Outward, Straight, Inward, respectively; see Figure 1). Based on the fingertip position data provided by the draw-wire potentiometer, interception was defined as being within a 3-cm range around the middle of the target arrival position, taken with respect to the middle of the index-finger. Participants were provided with this feedback immediately after each trial, which could either be "intercepted", "missed at left side", or "missed at right side", depending on performance.

Design

The reaching and interception tasks were performed in separate blocks, with task order randomized across participants. In the reaching task, participants performed 30 trials for each goal target position condition, presented in randomized order, resulting in a total of 90 reaching trials per participant. In the interception task, participants performed 30 trials under each combination of angle of approach and goal target arrival position conditions, presented in randomized order, resulting in a total of 270 interception trials per participant. The full experiment thus included 360 trials per participant.

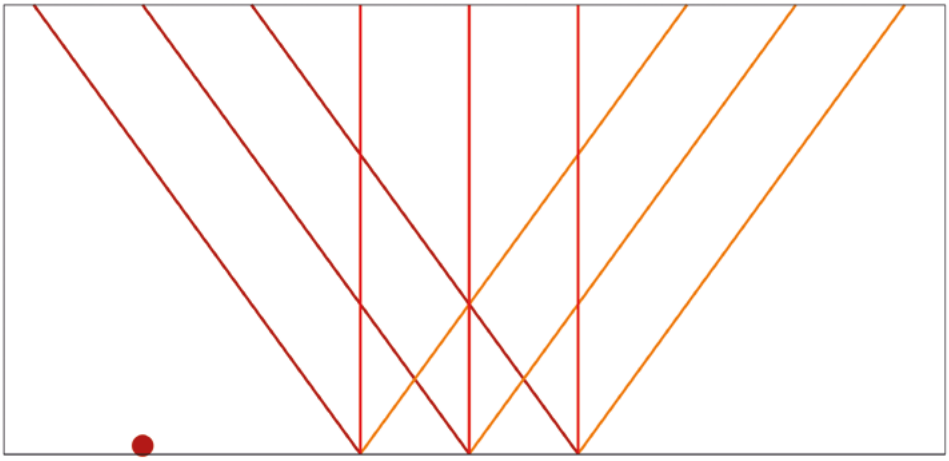

Figure 1. Target trajectories of the interception condition. The dot is the start target of the index finger, and the moving targets were intercepted along this lower lateral axis. The dark red (dark grey) lines are the -26.5° (outward) angle of approach, the red (grey) lines are the 0° (straight) angle of approach, and the orange (light grey) lines are the 26.5° (inward) angle of approach of the moving targets.

Data analysis

The data were analyzed using customized programs written in Matlab (Mathworks, Natick, MA). The percentage of intercepted balls in the interception trials was calculated using the feedback that was given to the participants which was based on the draw-wire potentiometer data. Subsequently, missed interception trials were excluded from the analysis. After filtering the X-Y-Z time series of fingertip position with a cut-off frequency of 5 Hz (low-pass second-order Butterworth filter ran through twice to negate the phase shift), the lateral (Z) velocity was computed using a three-point central difference method. For each trial, the start of the movement was determined by searching backward in time, starting from peak velocity. The first data point where the velocity fell below a threshold of 5 cm/s was marked as the start of the movement. In the reaching trials, the end of the movement was marked as the first data point where the velocity fell below a threshold of 5 cm/s when searching forward from peak velocity. In interception trials, the instant of interception (the time instant where the goal target passed the near end of the screen, 1 s after the target started moving) was marked as the end of the movement. Movement Time was defined as the time between the start and the end of the movement. The Variable Error of the end-effector was computed as the standard deviation of the difference between the end-effector lateral position at the end of the movement and the lateral position of the middle of the target (arrival) position. For the kinematic analysis, the uncontrolled manifold analysis and the joint deviation analysis (see upcoming sections) each trial was time-normalized to 100 steps, between the start and the end of the movement.

Kinematics

To statistically test differences in kinematics, we analyzed Movement Time and Symmetry Index of Velocity, which was defined as the time needed to reach peak velocity divided by Movement Time.

Synergistic organization of joint angles: UCM analysis

Joint rotations were computed following International Society of Biomechanics (ISB) guidelines for the upper extremity [68]: shoulder plane of elevation, shoulder elevation, shoulder inward–outward rotation, elbow flexion–extension, forearm pronation–supination, wrist flexion–extension, wrist abduction–adduction, index-finger flexion–extension, and index-finger abduction–adduction. The UCM method requires four steps [4]. As first two steps, the elemental variables selected were the nine joint angles while the 3D position of the tip of the index finger was selected as the performance variable. Subsequently, small changes in the joint angles were related to small changes in the index-finger position by means of a linear model (third step) and were represented in a Jacobian matrix. Lastly, this matrix was used to partition the joint-angle variance across trials; V_{ucm} is the variance within the null space of the Jacobian (i.e., variability in joint angles not affecting end-effector position) and V_{ort} is the variance orthogonal to the null space (i.e., variability in joint angles affecting end-effector position). Each UCM (V_{ucm} and V_{ort}) component was normalized by its number of DOF, and computed for each condition and each target (arrival) location separately. For the equations used in these four computational steps, see chapter 3. If V_{ucm} is larger than V_{ort}, there is mainly co-variation amongst joint angles. The relation between these two variables reflects the degree of co-variation. To correct for non-normal data distribution V_{ucm} and V_{ort} were log transformed prior to the statistical analysis [71].

Clusters of joint angle configurations

The goal of the current analyses was to establish whether different tasks and different conditions were performed with different synergies. To this end, we compared whether the cluster of joint angle configurations used in a base condition differed from that in the other conditions. We chose the Interception Straight (IS) condition as the base condition, to enable comparison of interception to reaching and to compare the different interception conditions[2]. All the computations reported hereafter were performed separately for each (distance) condition of each participant. First, we selected the null-spaces and orthogonal spaces of the Jacobian of the base conditions calculated for the UCM analysis as the bases. Then, joint deviation vectors (JDVs) were computed as the real difference between the average joint angle configuration of the base condition and the average joint angle configuration of each of the remaining (Reaching (R), Interception Outward (IO), Interception Inward (II) conditions (see [87]). These JDVs were projected onto the null-space of the base Jacobian and onto its orthogonal complement, resulting in the measures PR_{ucm}, PIO_{ucm}, PII_{ucm}, PR_{ort}, PIO_{ort}, PII_{ort}, respectively. The length of the projection onto the base null-space represents an estimate of the change in the joint angle configurations as a result of the change in task constraints between the base and the projected condition, which did not affect the fingertip position (P_{ucm}). The length of the projection onto the base orthogonal-space represents an estimate of that change that does influence the fingertip position (P_{ort}). Each projection component was normalized by the square root of its number of DOF [87]. These measures give an indication of the distance of the average joint angle configuration of a condition to the base condition, for both the null-space and the orthogonal space.

2 Note that the other conditions could also be used as a base condition. We performed those analyses and found similar results. Therefore we choose to present here only the analyses with the interception 0 as a base condition.

To establish whether synergies in fact differed between two conditions we computed a benchmark for the base condition to which the other conditions were compared. To compute the benchmark for the base condition we computed the difference between the joint angle configurations of the individual base trials and the average joint angle configuration of the base. We projected these on the null-space and orthogonal-space of the base condition. This resulted in the lengths of the projections of the deviation from the mean for each separate trial (of the base condition) in the null-space and orthogonal-space for the base condition. Again, these lengths were normalized by the square root of their number of DOF. Using the lengths of these projections, we calculated the upper bound of the 95% confidence interval for the projections onto the null space and the orthogonal space, which were chosen to represent the boundaries of the base synergy. Note that we did not use the lower bound of the confidence interval, because it is very close to the null space, as the null space is computed using small changes in the mean joint angle configuration of the base condition. Hence, the lower bound does not inform about the boundary of the base condition. We refer to these upper bounds as the projection bases (PB_{ucm} and PB_{ort}). The core of the analyses is comparing PB to the PR, PIO, and PII separately for each space (UCM and ORT) to establish differences between clusters of joint angle configurations (i.e., synergies), which we turn to now. Therefore, we tested whether the PR, PIO, and PII were larger than the boundary of the confidence interval of the PB, for each space separately (UCM and ORT). In the case that PR, PIO, or PII was larger than PB for both spaces, we interpreted this as the usage of a different cluster of joint angle configurations than that of the base condition, that is, a different synergy. It is important to realize that the main variables in this analysis are the lengths of projection vectors, whereas in the UCM analysis the variances of these vectors are the computed.

Statistical analysis

Variable Error and Movement Time were submitted to repeated measures ANOVAs with Condition (R, IS, IO, II) and Distance (20, 30, 40 cm) as within-participant factors. Symmetry Index of Velocity was submitted to a repeated measures ANOVA with Condition (R, IS, IO, II) and Distance (20, 30, 40 cm) as within-participant factors. This analysis was followed by two planned comparisons whether the deceleration tail was longer in interception compared to reaching, and the angle-of-approach effect in interception. The first preplanned contrast compared reaching to all three interception conditions and the second preplanned contrast compared IO to II.

To assess whether joint angles were organized in synergies, $V_{ucm}{}^{log}$, and $V_{ort}{}^{log}$ were submitted to a repeated measures ANOVA with Type of Variance ($V_{ucm}{}^{log}$, $V_{ort}{}^{log}$), Instant (33, 66, 100%), Condition (R, IS, IO, II), and Distance (20, 30, 40 cm) as within participant factors. To compare the synergies over conditions, we performed a repeated measures ANOVA with Space (UCM, ORT), Instant (33, 66, 100%), Projection (PB, PIO, PII, PR), and Distance (20, 30, 40 cm) as within participant factors. This analysis was followed by two preplanned comparisons that examined whether in reaching and in the other interception conditions different synergies emerge as in the base condition. The first planned contrasts compared the base projections to the projections of the IN and IP conditions for both UCM and ORT. The second planned contrast compared the base projections to the projections of the reaching condition for both UCM and ORT.

Effect sizes were calculated using generalized eta-squared statistics and interpreted as recommended: 0.02 for a small intensity effect, 0.13 for a medium intensity effect, and 0.26 for a large intensity effect [95]. Significant results with effect sizes smaller than 0.02 are not discussed. Where no planned comparisons were performed and further analyses were appropriate, significant ($p < 0.05$) main effects and interactions were analyzed using Newman-Keuls post-hoc tests.

Results

Due to (partial) occlusion of the markers or too early initiation of the movement in interception (prior to 150 ms after the goal target started moving), 3.5% percent of the trials were discarded. Interception performance was fairly good, with 82.5% of the targets being intercepted. All other dependent variables, including VE, were computed on intercepted trials only. As a result, the analyses concerned 1268 of the total 1350 trials in the reaching task and 3247 of the total 4050 trials in the interception task.

With an overall average of 0.7 cm, Variable Error was small relative to the available 3-cm margin at the target. The ANOVA on Variable Error nevertheless revealed a significant (but small intensity) main effects of Condition ($F(3,42) = 2.83$, $p = 0.049$, $\eta_g^2 = 0.08$) and Distance ($F(2,28) = 5.41$, $p = 0.01$, $\eta_g^2 = 0.03$), as well as a significant interaction of the two ($F(6,84) = 2.48$, $p = 0.029$, $\eta_g^2 = 0.05$). The interaction indicated that the differences in Variable Error across the tasks were more pronounced at a target distance of 20 cm and 40 cm than at a distance of 30 cm. Even though Variable Error varied to a certain extent between conditions, it´s amount consistently remained small with respect to the task requirements, indicating that overall movements were performed quite accurately.

Kinematics

Movement Time across all conditions was 0.65±0.002 s. The ANOVA on Movement Time revealed significant main effects of Condition ($F(3,42) = 106.08$, $p < 0.001$, $\eta_g^2 = 0.78$) and Distance ($F(2,28) = 132.89$, $p < 0.001$, $\eta_g^2 = 0.11$), and a significant interaction effect of the two ($F(6,84) = 18.48$, $p < 0.001$, $\eta_g^2 = 0.05$). Post hoc tests on the interaction revealed that Movement Time was shorter in reaching (0.48 s) compared to all interception conditions (IS: 0.73 s; IO: 0.71 s; II: 0.72 s; *p's* < 0.001). In addition, in reaching Movement Time increased with distance (20cm: 0.43 s; 30 cm: 0.49 s; 40 cm: 0.52 s) whereas in interception Movement Time was not affected by distance (*p's* < 0.05).

The ANOVA on Symmetry Index of Velocity (see Figure 2) revealed a significant main effect of Condition ($F(3,42) = 34.58$, $p < 0.001$, $\eta_g^2 = 0.4$), Distance ($F(2,28) = 20.78$, $p < 0.001$, $\eta_g^2 = 0.06$), and an interaction effect of the two ($F(6,84) = 6.24$, $p < 0.001$, $\eta_g^2 = 0.02$). The preplanned contrast comparing reaching to interception revealed that peak velocity occurred earlier in interception compared to reaching ($p < 0.001$), implying that the velocity patterns in interception had a longer decelerative tail. The preplanned contrast comparing IO and II revealed that peak velocity occurred later in the IO than II condition ($p < 0.05$), indicating an angle-of-approach effect.

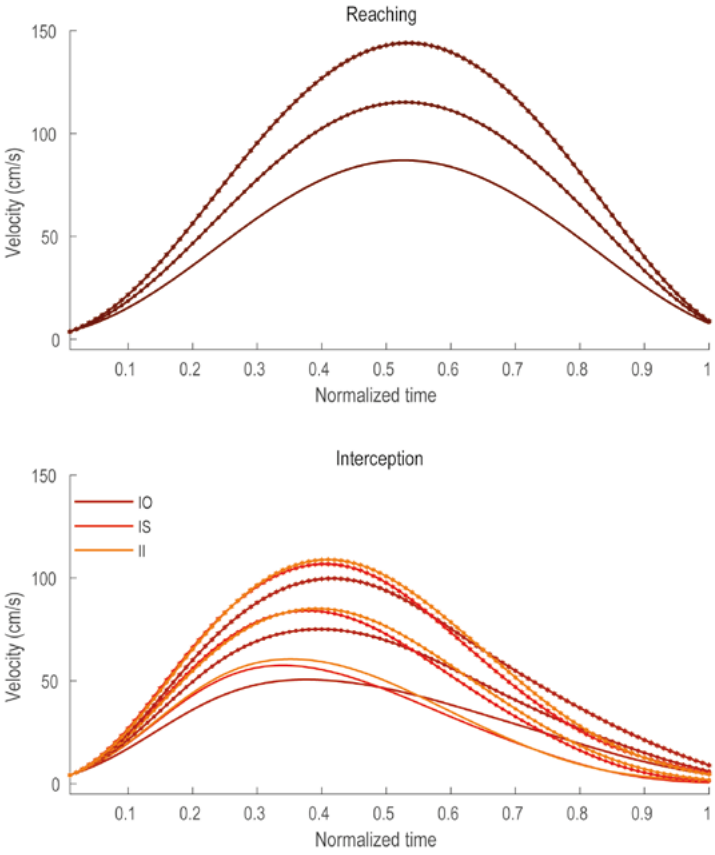

Figure 2. Mean velocity patterns of all conditions. Panel A shows the mean velocity patterns of each reaching condition. The lowest pattern corresponds to the 20 cm distance, the middle lightly dotted pattern to the 30 cm distance, and the upper dotted pattern to the 40 cm distance. Panel B shows the mean velocity patterns of the interception condition. R is reaching, IS is interception straight, IO is interception outward and II is interception inward.

Synergistic organization of joint angles: UCM analysis

The ANOVA on V_{ucm} and V_{ort} (see Figure 3) revealed a significant main effect of Type of Variance ($F(1,14) = 377.18$, $p < 0.001$, $\eta_g^2 = 0.69$) and a significant main effect of Condition ($F(3,42) = 11.65$, $p < 0.001$, $\eta_g^2 = 0.06$). No effects for Instant or other effects were significant. The main effect of Type of Variance indicated that V_{ucm} was always larger than V_{ort}, which implies DOF were organized in synergies in all experimental conditions. Type of Variance did not interact with other factors implying that the degree of co-variation did not differ amongst conditions. Post hoc tests on the main effect of Condition revealed that both types of variance were higher in all interception conditions compared to reaching (p's < 0.001), indicating that the joint angle variance is higher in interception.

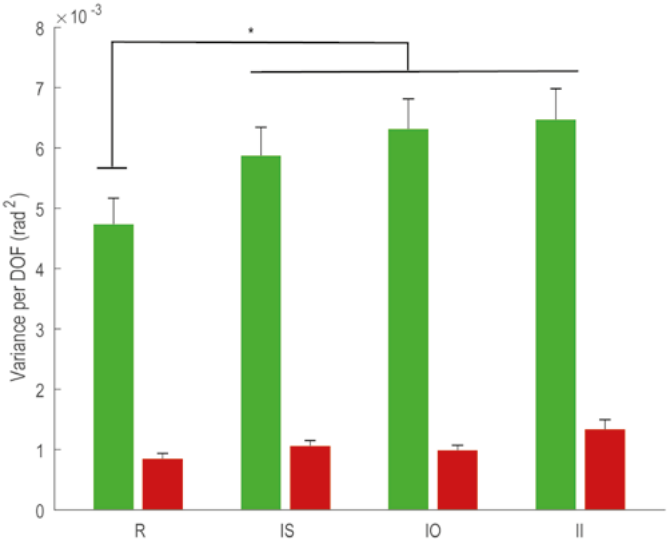

Figure 3. Mean Joint Angle Variance patterns over time. The green (grey) bars are V_{ucm} and the red (dark grey) bars are V_{ort}. R is reaching, IS is interception straight, IO is interception outward and II is interception inward. Note that the error bars denote the standard error of the mean. An asterisk denotes a significant difference.

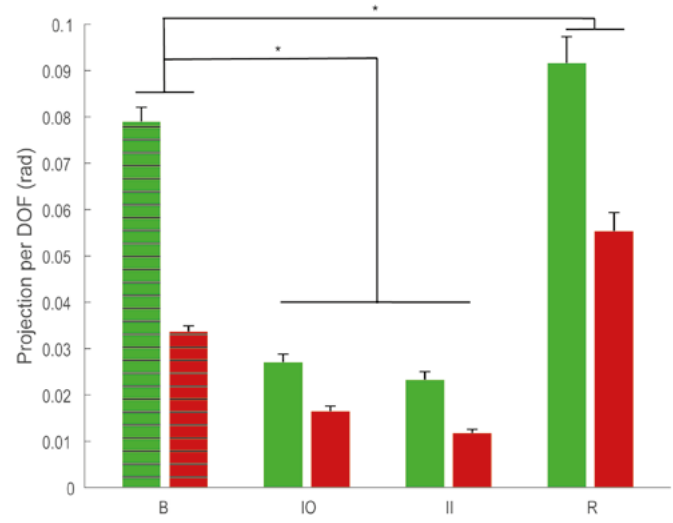

Figure 4. Mean Joint Vector Projection Patterns. The green (dark grey) bars are $Projection_{ucm}$ and the red (grey) bars are $Projection_{ort}$. Note that the base condition is the upper bound of the confidence interval of each trials with respect to the mean, whereas the other conditions are the mean difference between the condition and the base. B is the base (Interception Straight), IO is interception outward, II is interception inward and R is reaching. Note that the error bars denote the standard error of the mean. An asterisk denotes a significant difference.

Clusters of joint angle configurations

The ANOVA on the projections (see Figure 4) revealed significant main effects of Space ($F(1,14) = 78.8$, $p < 0.001$, $\eta_g^2 = 0.30$) and Projection ($F(3,42) = 70.9$, $p < 0.001$, $\eta_g^2 = 0.58$), and a significant interaction effect of these two factors ($F(3,42) = 26.3$, $p < 0.001$, $\eta_g^2 = 0.13$). No effects for Instant or other effects were significant. The effect of Space denotes that the projections in the UCM space were larger than the projections in ORT space, as found by Mattos and collegueas and Schöner [87,114]. The first preplanned contrast revealed that the projections of the interception inward and outward conditions were shorter than the base projections for both UCM and ORT spaces ($p's < 0.001$), implying no differences in the clusters of joint angle configurations used. The second preplanned contrast indicated that the projections of the reaching conditions were longer than the base projections, for both UCM and ORT spaces ($p's < 0.05$), implying the usage of different clusters of joint angle configurations. Taken together, these results suggest that the synergistic organization of DOF did not differ among interception conditions, whereas synergies were different between reaching and interception.

Discussion

The current study focused on emergent synergies and aimed to establish whether different synergies emerge as a function of task constraints. Synergies were characterized by the degree of co-variation amongst joint angles across repetitions and by the cluster of joint angle configurations employed by the synergy. Synergies can change if task constraints vary, and we assumed that task constraints affect synergies and end-effector kinematics independently, as proposed by Kay [10]. To determine which variations in task constraints affected synergies only, we examined both synergies and end-effector kinematics. To do this, we used different conditions of manual reaching and manual interception in our experiment of which differences in end-effector kinematics could be expected based on earlier studies (e.g., compare [51] to [53]). Our findings confirmed these differences, demonstrating that the velocity profile of the end-effector was roughly symmetric in manual reaching, whereas in manual lateral interception it had a longer decelerative tail. In addition, the velocity profile showed an angle-of-approach effect in interception. Subsequently, our results demonstrated that the joint angle configurations exhibited primarily co-variation instead of other variation in all conditions, indicating that joint angles were organized in synergies. The key finding of the current paper is that amongst interception conditions no differences in the clusters of joint angle configurations were found, whereas between reaching and interception the employed clusters of joint angle configurations differed. In the current study this was interpreted as that emergent synergies were different between reaching and interception, whereas amongst interception conditions similar synergies emerged. Taken together, these results imply that some task constraints operate at the level of synergies while other task constraints only affect kinematics, which is in line with the suggestion of Kay [10]. That is, the interaction of constraint leads to the production of goal-directed behavior, but, depending on the specifics of the constraints in some cases different synergies emerge while in other cases a similar synergy is constrained differently, both producing various kinematic patterns at the end-effector level.

Our findings regarding the end-effector kinematics are in line with the literature. As in previous studies [51,52,108] we found that the velocity profile in reaching is roughly bell-shaped. Furthermore, the velocity profile in manual interception was asymmetric with a longer deceleration tail and showed an angle-of-approach effect, an effect also established in earlier studies [53–56], implying systematic differences between targets moving inward (i.e., with the lateral component of the target trajectory moving toward the participant) and moving outward (i.e., with the lateral component of the target trajectory moving away from the participant). More specifically, the moment of peak velocity occurred earlier for the inward moving targets compared to the outward moving targets. All our findings regarding the kinematics of the end-effector are concurrent with earlier findings [53–56], however, the current paper is to our knowledge the first to make a direct end-effector kinematics comparison between reaching and interception, and confirms the presumed differences.

With respect to the synergistic organization of joint angles, ample literature has revealed that in manual reaching V_{ucm} was larger than V_{ort} (see also [31,32,37,38,43,66,115–118,123]). This was also revealed in our reaching conditions, implying that DOF were organized in synergies. A novel contribution to the literature is that V_{ucm} was also larger than V_{ort} in a manual lateral interception task. This supports earlier findings indicating that joint angles are coordinated in synergies in unrestrained catching [120,121], using other methods of analysis than a UCM analysis. Moreover, we found that both V_{ucm} and V_{ort} were higher in interception compared to reaching, showing that joint angle coordination patterns were more variable in interception than in reaching. Importantly, the type of variance (i.e., V_{ucm} and V_{ort}) did not interact with other factors, which indicated that the degree of co-variation did not differ amongst conditions, implying that the coupling strength among DOF within the synergies of those tasks did not differ.

Our most important finding was that some task constraints (i.e., differences between reaching and interception) affected synergies, whereas other task constraints (i.e., angle of approach) did not affect synergies but were involved in constraining synergies, thereby affecting end-effector kinematics. This finding is based on the revealed differences in clusters of joint angle configurations between reaching and interception, whereas no differences in clusters of joint angle configurations were found amongst interception conditions. Interestingly, the end-effector kinematics did differ between reaching and interception and amongst interception conditions with different angles of approach. We interpret these findings as support for the two-step process of constraining DOF as proposed by Kay [10]. Kay argued that the emergence of a synergy is the first step in the constraining process. This synergy takes the form of a dynamical system [20,124–126], of which the properties are characterized by the specifics of an attractor. An attractor can be defined as a set of states where a system tends to evolve towards. Such an attractor generates a cluster of joint angle configurations with a certain size and location in joint space that reflect the synergy. The second step of the process is the additional constraining of the attractor leading to the production of the actual movement [10]. It has also been suggested that this two-step process is at play in interpersonal coordination [26,31], suggesting that this process coordinates DOF at different behavioral levels.

Our results illustrate a hallmark of the dynamical systems approach, that is, there is structure in variability that characterizes the attractor reflecting the organization of the DOF (cf. [29]). In doing so, we studied structure in variability at the level of the joint angles and how it relates to variability at the end-effector level [4,5,127]. Our analyses focusing on two levels add to the usual dynamical systems analyses that characterizes the attractor at just the end-effector level [19,21,128–130]. Coordination at the joint angle level in the arm was also studied from a dynamic systems perspective. That is, Buchanan et al. [131] analyzed changes in relative phase relations between wrist, elbow, and shoulder joints under systematic variation of curvature of end-effector movements. However, relative phase is computed between two angles. To understand coordination amongst more than two angles as well as the relation between joint angle variability and end-effector variability, a different technique is required. For that reason, we followed studies in interpersonal coordination [26,31] and in motor development [115,119], and employed the UCM analysis in the current study.

Applying the UCM analysis and its extended techniques to assess coordination amongst more DOF might also be employed to understand how emergent synergies deal with perturbations in future studies. That is, a key example of synergistic organization of DOF is an experiment on speech production where participants were asked to produce a specific syllable, while during the production of this syllable the lower lip was mechanically perturbed [18]. Interestingly, during the perturbation the production of the syllable was preserved through instantaneous changes in the movements of the upper lip, lower lip, or tongue, depending on the syllable (i.e., motor equivalence). Over the years, other studies also showed adjustments in DOF other than the one perturbed to maintain the function of the synergy [18,27,28,132–134]. Note that these studies focus on a limited number of DOF to understand how the synergy maintains its function after a perturbation. A study employing UCM analyses and one of its extensions, that is, motor equivalence analysis, showed that the collective DOF adjust (i.e., most changes in joint angle configurations were motor equivalent) after a perturbation of the elbow when an elastic band gently pulled at the elbow during reaching [87]. This implies that current techniques can examine how the collective DOF are coordinated to maintain the function of the synergy. Exploiting these techniques in future studies would elevate our understanding of the process of the emergence of synergies by understanding how a large set of DOF contributes to meet task demands under perturbations.

With respect to the employed analyses techniques used to examining the cluster of joint angle configurations, we applied a modified version of a UCM based method to analyze motor equivalence [87,114]. Schöner's method to show motor equivalence computed projection lengths of a perturbed condition on the UCM of an unperturbed condition. Actions were considered motor equivalent if those projection lengths were larger in the UCM space compared to the orthogonal space (note that all conditions of the current study were motor equivalent). This analysis inspired our analysis to assess differences in synergies, where we looked at differences in projection lengths within UCM and ORT space, respectively. With this adapted version of the UCM analysis we quantified the location and the size in joint space of a cluster of joint angle configurations, which we take to reflect the joint angle configuration employed by the synergy.

The dynamic systems approach to motor coordination is one view on how the abundant DOF in the neuromotor system could be organized in synergies. Another influential approach is the muscle synergies perspective (cf. [12,14,135,136]). Muscle synergies are modules in the neuromotor system where each module activates a certain set of muscles in a fixed proportional way. To produce a movement the neuromotor system activates these modules over time and varies the activation level of the modules to generate different movements (see [111] for an recent in-depth overview). In this approach, variability in the muscle activation patterns [12,135] originates from variations in the activation signals, which might stem from a change in the command signal or from noise in the system (cf. [137]). How task constraints could affect these synergies has been addressed in a study of D'Andola et al. [138], arguing that variability in muscle activation patterns originated from differences in activation of muscle synergies between reaching and one-handed unrestrained catching. However, it is difficult to establish how this finding relates to our findings because of the differences in underlying starting point in understanding motor control. For instance, in the muscle synergy approach noise is an important source of variability, while we take the structure in variability to be informative about the actual synergy organizing DOF. In that light it is unclear to us how our finding of primarily co-variation can be explained from a muscle synergy perspective.

In conclusion, the current study examined whether different synergies emerged when task constraints were varied in manual reaching and a manual interception. We found that although kinematic profiles differed among all conditions, synergies only varied between reaching and interception, but not among interception conditions. Together these results support the two-step process as proposed by Kay [10] to coordinate the redundant DOF in the action system.